Circular Dichroism Spectroscopy Is a Sensitive Tool for Investigation of Bilirubin−Enzyme Interactions

ARTICLE *in* BIOMACROMOLECULES · JANUARY 2011

Impact Factor: 5.75 · DOI: 10.1021/bm1012103 · Source: PubMed

1 AUTHOR:

Ferenc Zsila
Institute of Materials and Environmental C…

94 PUBLICATIONS **1,867** CITATIONS

SEE PROFILE

Circular Dichroism Spectroscopy Is a Sensitive Tool for Investigation of Bilirubin−Enzyme Interactions

Ferenc Zsila*

Department of Molecular Pharmacology, Institute of Biomolecular Chemistry, Chemical Research Center, H-1025 Budapest, Pusztaszeri út 59-67, Hungary

Received October 11, 2010; Revised Manuscript Received November 10, 2010

Noncovalent complex formation of unconjugated bilirubin with various enzymes has been demonstrated by measuring induced circular dichroism (ICD) peaks associated with the pigment VIS absorption band. Preferential binding of the *P*- or *M*-helical conformer of bilirubin to dehydrogenases, catalase, alkaline phosphatase, and α-chymotrypsin is responsible for the characteristic exciton CD couplet that undergoes remarkable changes upon the addition of enzymatic cofactors (NADH, AMP) and an inhibitor (acridine). Alterations of the ICD spectra refer to a direct binding competition between bilirubin and NADH for a common binding site on alcohol dehydrogenase and catalase, suggesting a potential mechanism for the inhibitory effect of BR reported on NAD(P)H dependent enzymes. NADH and bilirubin form a ternary complex with glutamate dehydrogenase indicated by peculiar CD spectral changes that are proposed to be generated by allosteric mechanism. α-chymotrypsin binds bilirubin in its catalytic site, as indicated by CD displacement experiments performed with the competitive inhibitor acridine. Surprisingly, the closely related trypsin does not induce any CD signal with bilirubin. Taking into consideration the clinically relevant but controversial and poorly understood areas of bilirubin biochemistry, the fast and simple CD spectroscopic approach presented here may help to unfold diverse physiological and pathophysiological roles of BR on a molecular level.

Introduction

The yellow-orange pigment of jaundice (4*Z*,15*Z*)-bilirubin-IXα is produced abundantly in mammals by catabolism of heme and transported to the liver for glucuronidation and excretion.[1] Bilirubin (BR) is an acyclic tetrapyrrole that consists of two rigid, planar dipyrrole units (dipyrrinones) joined by a methylene bridge at C_{10}. BR can fold into either of two enantiomeric conformations that minimize steric repulsions and are stabilized by six intramolecular H-bonds between the propanoic acid carboxyl groups at C_8 and C_{12} and the opposing dipyrrinone lactam and pyrrole NH−C═O groups (Figure 1). These isoenergetic, "ridge-tile" conformations are nonsuperimposable mirror-images, and the interconversion rate between them is known to be fairly rapid at room temperature.[2,3] Therefore, in isotropic solvents, BR does not exhibit any intrinsic optical activity, but its interaction with chiral complexing agents (e.g., proteins) leads to the observation of two main proximate bands of opposite sign called Cotton effects (CEs) in the circular dichroism (CD) spectrum. Such a bisignate CD profile of BR−host complexes is interpreted by the exciton mechanism, that is, the intramolecular dipole−dipole coupling between the electronic transition moments of the two dipyrrinone chromophores juxtaposed in a specific dissymmetric conformation.[2,3] The signed order of the CD exciton couplet is determined by the relative helicity of the transition dipole moments of the dipyrrinone moieties indicating the prevalence of the *P*- or *M*-helical conformation of the BR molecule at the asymmetric binding site. In contrast with the large amount of work in CD and absorption spectroscopic investigations of serum albumin binding of BR,[2,4−8] only very few attempts have been made to explore and characterize BR−enzyme interactions.[9,10] In vitro BR shows widespread inhibitory effects on a number of various, NAD(P)H-dependent/independent enzymes,[11−15] uncouples oxidative phosphorylation in mitochondria,[16,17] and inhibits protein kinases, too.[18] These are important issues due to the BR encephalopathy[11,19] and the recently recognized role of BR in the pathogenesis of several nonhepatic diseases,[20] specific nature, and underlying mechanisms of which are still largely unknown. Therefore, the present study is aimed to demonstrate the multifaceted use of CD spectroscopy for quick, simple and informative investigation of binding of BR to various enzymes, in vitro inhibition of which by BR has previously been reported (except for catalase): α-chymotrypsin (CHT),[11,13] alcohol dehydrogenase (ALDH),[21] L-glutamate dehydrogenase (GLDH),[22] catalase (CTL), and placental alkaline phosphatase (ALP).[11] The induced CD (ICD) spectrum of enzyme-bound BR also enabled us to study

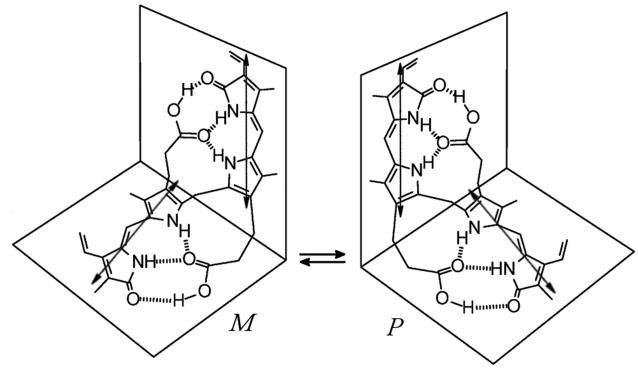

Figure 1. Ridge-tile shape *M*- and *P*-helicity intramolecularly hydrogen-bonded interconverting conformers of bilirubin. Double-headed arrows represent the electronic transition dipole moments polarized along the long axis of the dipyrrinone chromophores. For the *M*-conformer, chiral exciton coupling of the transition moments results in a longer-wavelength negative and a shorter-wavelength positive CE in the CD spectrum. (CD bands are inverted for the *P*-conformer.)

* Corresponding author. Fax: (+36) 1-438-1145. E-mail: zsferi@chemres.hu.

10.1021/bm1012103
Published on Web 12/08/2010

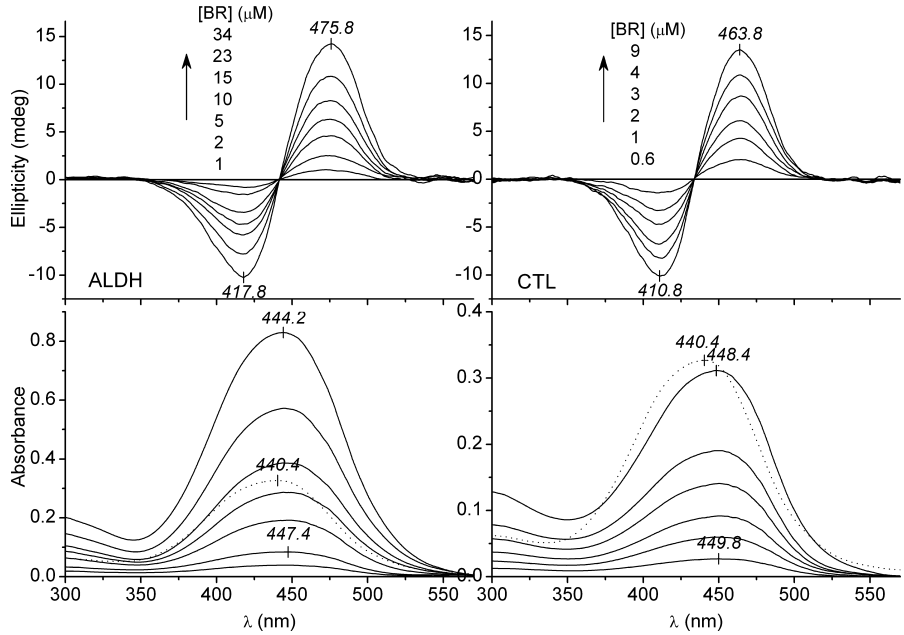

Figure 2. Selected difference CD and absorption spectra obtained by titration of ALDH (34 μM) and CTL (26 μM) with incremental addition of BR (Ringer buffer, $t = 25$ °C). Dotted line: absorption spectrum of 10 μM BR in Ringer buffer at 25 °C.

BR−coenzyme binding interactions showing direct competitive as well as allosteric effects. Additionally, it has become apparent that CD spectroscopy can be a very sensitive tool for differentiating among structurally very similar enzymes such as trypsin (TRP) and chymotrypsin.

Experimental Methods

Materials. Bilirubin (BR, bilirubin-IXα: 88%, bilirubin-XIIIα: 5%, bilirubin-IIIα: 7%), β-nicotinamide adenine dinucleotide (reduced disodium salt hydrate, 97%), acridine (ACR, 99.1%), adenosine 5′-monophosphate disodium salt (AMP, 99.8%), alkaline phosphatase from human placenta (type XXIV, 17 units/mg solid), α-chymotrypsin from bovine pancreas (type II, protein content = 97%; 59 units/mg protein), catalase from bovine liver (protein content = 79%; ≥10 000 units/mg protein), L-glutamate dehydrogenase from bovine liver (type II, 40 units/mg protein), and trypsin from bovine pancreas (protein content = 99%; 13 961 BAEE units/mg protein) were purchased from Sigma. Alcohol dehydrogenase from yeast (protein content = 96%; 300 units/mg protein) was obtained from Worthington Biochemical Corporation. All protein samples were used as supplied. All other chemicals were of analytical grade.

Preparation of BR and Enzyme Solutions. Stock solutions of BR (normally about 5×10^{-4} to 1×10^{-3} M) were prepared freshly by dissolution of BR in 0.005 M aqueous NaOH. Protein samples were dissolved in physiological Ringer buffer solution (pH 7.4, 137 mM NaCl, 2.7 mM KCl, 0.8 mM $CaCl_2$, 1.1 mM $MgCl_2$, 1.5 mM KH_2PO_4, 8.1 mM $Na_2HPO_4 \cdot 12H_2O$, and 1.5 mM NaN_3) or in 0.1 M Tris-HCl buffer, pH 8.0 (0.1 M NaCl). Subunit molar concentrations of the enzymes were calculated from weight by taking into consideration purity data provided by the supplier.

Circular Dichroism and UV/vis Absorption Spectroscopy Measurements. CD and UV/vis spectra were recorded on a Jasco J-715 spectropolarimeter at 25 ± 0.2 °C. Temperature control was provided by a Peltier thermostat equipped with magnetic stirring. For recording CD spectra, rectangular quartz cells of 1 or 0.5 cm (Figure 4) optical path length were used. Each spectrum represents the average of three scans obtained by collecting data at a scan speed of 100 nm/min. UV/vis absorption spectra were obtained by conversion of the high voltage (HT) values of the photomultiplier tube of the CD equipment into absorbance units. CD and absorption curves of BR−enzyme mixtures were corrected by subtracting the spectra of enzymes. JASCO CD spectropolarimeters record CD data as ellipticity (Θ) in units of millidegrees (mdeg). The quantity of Θ is converted to $\Delta\varepsilon$ values using the equation $\Delta\varepsilon = \Theta/(32\,982cl)$, where $\Delta\varepsilon$ is the molar circular dichroic absorption coefficient expressed in M^{-1} cm^{-1}, c is the molar concentration of the ligand (mol/L), and l is the optical path length expressed in centimeters.

Calculation of BR Binding Parameters from CD Data. Details of the estimation of the association constants (K_a) and the number of binding sites (n) using CD titration data have been previously described.[23] Nonlinear regression analysis of the ICD values measured at different [BR]/[enzyme] molar ratios was performed by the NLREG software (statistical analysis program, version 3.4 created by Philip H. Sherrod).

Results and Discussion

CD and Absorption Spectroscopic Investigation of Bilirubin−Enzyme Interactions. Figures 2 and 3 display representative difference CD and absorption curves of BR−enzyme complexes measured at increasing [BR]/[enzyme] molar ratios. Spectral positions and amplitudes in molar units of the ICD and absorption bands are shown in Table 1. Between 300 and 570 nm the absorption spectrum of BR in Ringer buffer solution exhibited a maximum around 440 nm. Because of its hydrophobic moieties and the internal H-bonding of all of its polar groups, the maximum aqueous solubility of BR is very low at pH 7.4; it is ~0.1 μM.[24] Thus, BR shows a strong tendency to form molecular aggregates in physiological buffer solutions, which results in a considerable hypochromism in the VIS absorption band in relation to strongly alkaline buffers in which BR dissolves much better (Table 1).[25] In the presence of the enzymes, however, the ε_{max} values did not show hypochromism, indicating that BR binds to the enzymes in a nonaggregated, monomeric form (Table 1). In addition, by a various extent, all enzymes caused a bathochromic shift of the VIS absorption maximum, which is a further characteristic sign of the formation of BR−protein complexes.[26,27] Except for ALP, all enzymes induced a typical bisignate exciton CD spectrum, similarly to that reported previously for serum albumins,[2,4−8] glutathion-*S*-

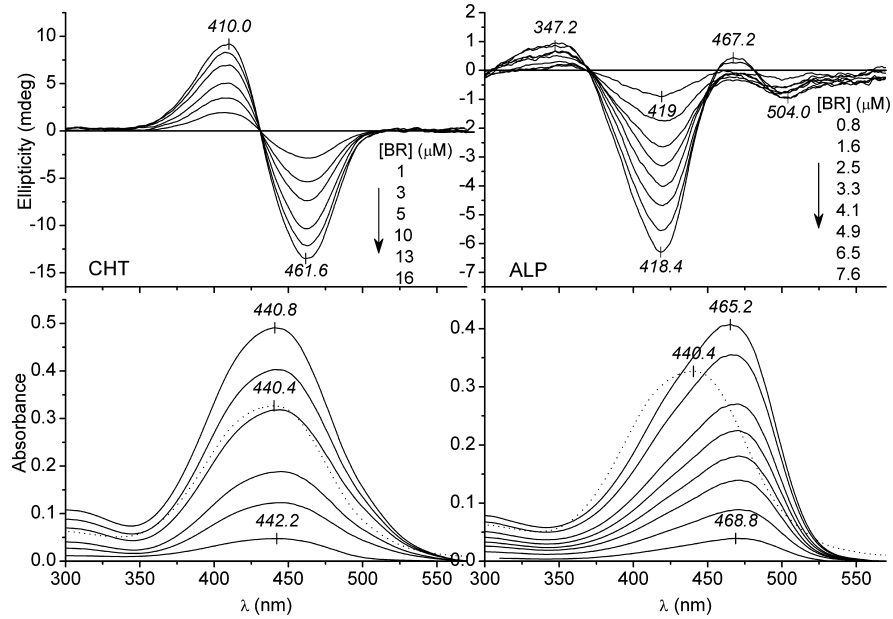

Figure 3. Selected difference CD and absorption spectra obtained by titration of CHT (34 μM) and ALP (30 μM) with incremental addition of BR (Ringer buffer, $t = 25$ °C). Dotted line: absorption spectrum of 10 μM BR in Ringer buffer at 25 °C.

Table 1. Molar CD ($\Delta\varepsilon$) and Absorption (ε) Extrema of BR−Enzyme Complexes in Ringer Buffer Solution at 25 °C[a]

enzyme	[enzyme] (μM)	[BR] (μM)	$\Delta\varepsilon_1$ ($M^{-1}cm^{-1}$)	$\Delta\varepsilon_2$ ($M^{-1}cm^{-1}$)	$\varepsilon_{max} \times 10^{-3}$ ($M^{-1}cm^{-1}$)
ALDH	34	2	−28 (417.8)	+46 (473.8)	51 (447.4)
GLDH	57	44	−3 (391.6)	+4 (442.0)	53 (444.8)[b]
CTL	26	3	−74 (410.2)	+95 (464.6)	51 (450.6)
CHT	34	1	+71 (407.2)	−105 (462.6)	54 (444.4)
ALP	30	4	+5 (349.6)	−30 (420.0)	55 (469.8)
				+6 (499.0)	
pH 7.4 Ringer		5			33 (441.0)
pH 9.8 Tris-HCl		5			49 (439.0)

[a] $\Delta\varepsilon$ and ε values were calculated by using BR concentrations of the sample solutions. λ_{max} values (nanometers) are given in parentheses. [b] Calculated from the absorption spectrum of 3 μM BR measured in the presence of 30 μM GLDH. ε_{max} values of BR obtained in pH 7.4 and 9.8 protein-free buffer solutions are shown.

transferase,[9] apomyoglobin,[10] and lipocalin proteins.[27−29] In the case of GLDH, only a single CD curve is displayed because the weak and noisy CEs did not allow us to collect quality CD spectra at lower [BR]/[enzyme] ratios (Figure 4). Such type of CD spectra is characteristic of intramolecular exciton coupling between the two dipyrrinone units of the bichromophoric pigment. According to the exciton chirality rule,[3,30] the signed order of the CEs indicates that the binding sites of ALDH, CTL, and GLDH prefer the *P*-helical conformation of BR, whereas the binding site of CHT favors the opposite, *M*-helical conformation of the pigment molecules (Figure 1). Comparison of the $\Delta\varepsilon_{max}$ values shows that the binding sites of CTL and CHT possess the largest stereoselectivity toward one helical conformation of BR.

In comparison with the bisignate CD spectra measured with other enzymes, the ICD curve of BR−ALP complexes is rather atypical showing multiple CEs (Figure 3). Two positive peaks are centered at 347 and 467 nm, whereas a major negative CE of increased intensity is situated around 419 nm. An additional long-wavelength negative ICD band appeared at 504 nm. Furthermore, in relation to other enzymes, ALP binding produced the largest by far, a 28 nm red shift in the λ_{max} value of BR (Figure 3, Table 1). Exciton interactions can alter not only the CD but also the absorption spectrum. When the ridge-tile conformation of BR unfolds in the direction of extended or

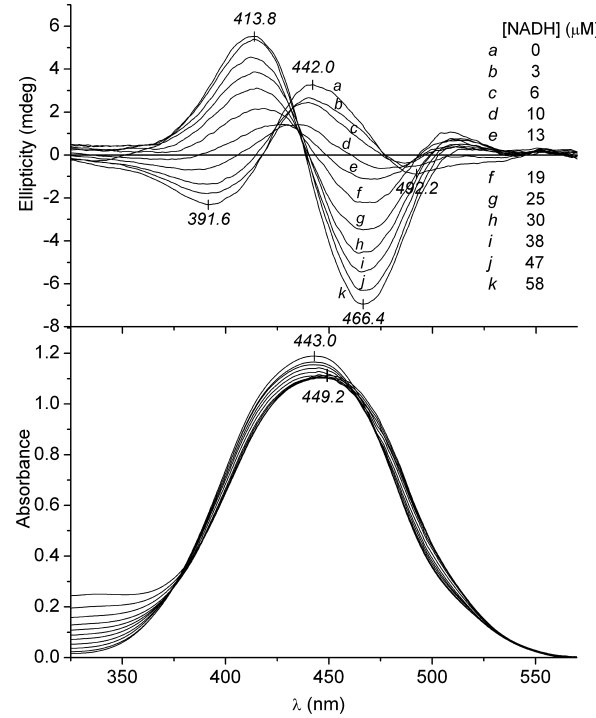

Figure 4. Changes of difference CD and absorption spectra of BR−GLDH (44 μM-57 μM) mixture upon addition of μL aliquots of 2 mM NADH stock solution (Ringer buffer, $t = 25$ °C, optical path length is 0.5 cm).

linear conformations, the transition dipoles of the dipyrrinone chromophores (Figure 1) tend to reorient toward parallel or in-line, resulting in the red shift of the VIS absorption.[3] Therefore, the large red shift suggests that in the ALP-bound state the ridge-tile conformation of BR is opened toward the extended form.

Calculation of BR Binding Parameters from the ICD Data. By assuming that the magnitudes of the ICD bands of BR are proportional to the protein-bound fraction of the pigment, nonlinear regression analysis of CD titration data of BR−enzyme complexes was performed to estimate the binding parameters, the apparent association constant (K_a), and the number of BR

Table 2. Binding Parameters of BR−enzyme Complexes Calculated from CD Titration Data[a]

enzyme	number of subunits	[enzyme] (μM)	[BR] (μM)	λ (nm)	K_a (M^{-1})	n	r^2
ALDH	4	34	70	475	4.2 ($\pm$0.5) $\times$ 10^5	0.1	0.9949
CTL	4	26	15	464	1.4 ($\pm$0.1) $\times$ 10^6	0.1	0.9977
		26	*42*	*464*	*1.3 ($\pm$0.3) $\times$ 10^6*	*0.3*	*0.9861*
CHT	1	34	47	462	1.9 ($\pm$0.5) $\times$ 10^5	0.1	0.9744
		34	*54*	*462*	*1.7 ($\pm$0.2) $\times$ 10^5*	*0.5*	*0.9914*
ALP	2	30	62	419	2.2 ($\pm$0.4) $\times$ 10^6	0.2	0.9978

[a] Enzyme and titration end-point concentrations of BR as well as wavelengths of the CD data collection (λ) are shown. Titrations were performed in pH 7.4 Ringer buffer solution at 25 °C. For CHT and CTL, titration procedures were repeated in 0.1 M Tris-HCl buffer, pH 8.0 containing 0.1 M NaCl (data in italic).

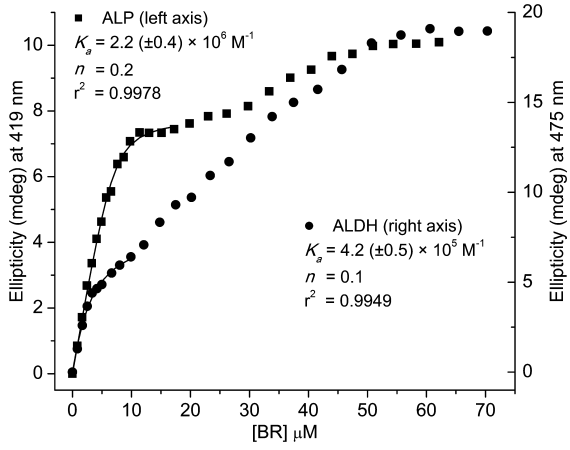

Figure 5. CD titration of 30 μM ALP and 34 μM ALDH with BR in Ringer buffer at 25 °C. Squares and circles: experimental CD data points. Solid lines: results of curve fitting-procedure.

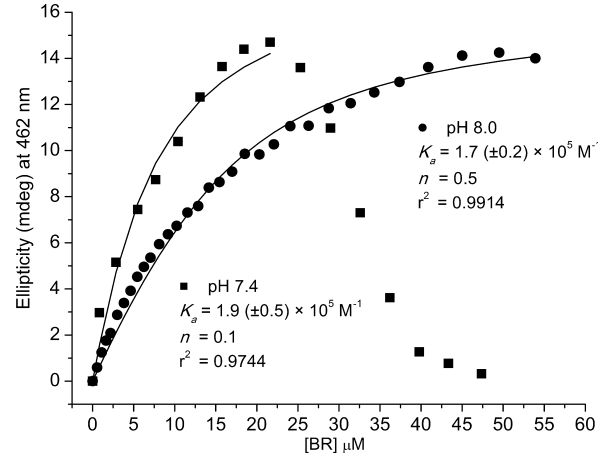

Figure 6. CD titrations of 33 μM CHT with BR in pH 7.4 Ringer and in Tris-HCl buffer, pH 8.0 (0.1 M NaCl) buffer solutions at 25 °C. Squares and circles: experimental CD data points. Solid lines: results of curve fitting-procedure.

binding sites per enzyme subunit (n).[23] Because GLDH induced low-intensity CD signals for BR (see curve "a" in Figure 4), no sufficient number of quality CD data could be collected for a reliable calculation. The K_a values obtained show that BR binds to CTL and ALP with the highest affinity, whereas the BR−ALDH and BR−CHT interactions are weaker by an order of magnitude (Table 2). Distinctly from CTL and CHT, titration curves of ALDH and ALP are composed from two well-separated parts: after an initial steep phase, the increment of the CD values decreases, giving rise to a second, flat section of the data points (Figure 5). For ALDH and ALP, the affinity constants were estimated by curve fitting on the first part of the CD titration data points. One interpretation of this result is the negative cooperativity between the BR binding sites of the enzyme subunits, but there is an alternative interpretation, too: it is due to the presence of independent noninteracting sites that have different affinities for BR. However, this is less plausible because the shape, λ_{max} values, and relative intensities of the ICD bands of BR−ALDH and BR−ALP complexes did not show variation during the titration procedures, from 1> [BR]/[enzyme] ratios to ~2. It is unlikely that the flexible structure of BR that is very sensitive to subtle topographical changes of the binding sites would give rise to identical ICD curves upon binding to distinct, different affinity sites. The very low n values obtained for BR binding sites per enzyme subunit (Table 2) could be due to the poor aqueous solubility of BR molecules at pH 7.4 (~0.1 μM). During the CD titrations, much higher BR concentrations than 0.1 μM must be used to collect sufficient number of data points for curve fitting (Figures 2 and 3, Table 2). As the titration proceeds, the unbound fraction of BR steadily increases and the BR molecules start to form aggregates that behave as nonspecific, CD inactive BR binding objects and compete for BR with the protein binding sites. In the early phase of the titration when the [BR]/[enzyme] ratio is low, this effect is negligible, but at higher BR concentrations, larger aggregates are formed that sequester more effectively the pigment molecules. Thus, the dynamic BR−enzyme ⇌ BR−aggregate equilibrium is shifted toward the aggregated state resulting quick saturation of the ICD values and thus underestimated stoichiometry. In an extreme case, especially when BR binds in a superficial solvent exposed protein site, increasing BR binding ability of the aggregates may cause the dissociation of the BR−enzyme complexes. This phenomenon was observed during the titration of CHT at pH 7.4: upon increase in BR concentration in the sample solution >20 μM ([CHT] = 34 μM), the ICD bands started to decrease and vanished completely upon reaching 47 μM (Figure 6). No such anomalous behavior could be observed; however, when the titration was performed in pH 8.0 Tris-HCl buffer, BR dissolved better and thus its aggregation tendency was suppressed in relation to the pH 7.4 Ringer buffer (Figure 6). Furthermore, the n value derived from this titration data is five times larger (Table 2), supporting the effect of BR aggregation in obtaining anomalously low stoichiometry values at physiological pH. It is of note that in contrast with the stoichiometry of the binding, values of the association constants calculated from CD titration data recorded at physiological and alkaline pH showed only minor alterations (Table 2), suggesting that the association constants estimated at pH 7.4 can be used to characterize the enzyme binding affinity of BR. Similar results were found when BR titration of CTL was repeated in pH 8.0 Tris-HCl buffer (Table 2).

Effects of Cofactors and Inhibitors on the CD and Absorption Spectra of Bilirubin−Enzyme Complexes. All enzymes except for CTL are optically transparent above 300 nm, and thus they do not contribute to either the CD or the UV/vis spectra. As a heme protein, however, CTL contains four protoporphyrin IX rings that are well buried in the tetramer, at

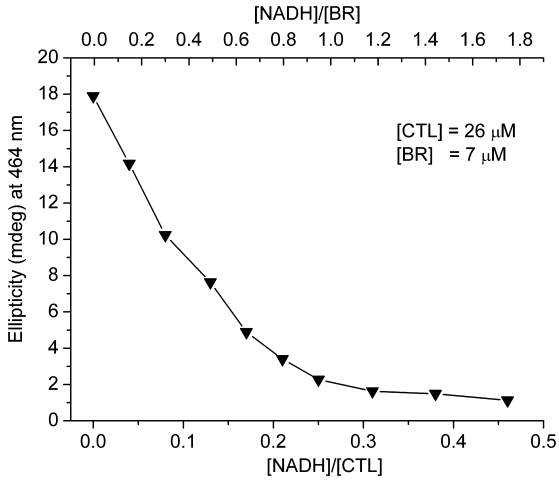

Figure 7. Effect of NADH on the positive ICD band of BR−CTL complexes (Ringer buffer, $t = 25$ °C).

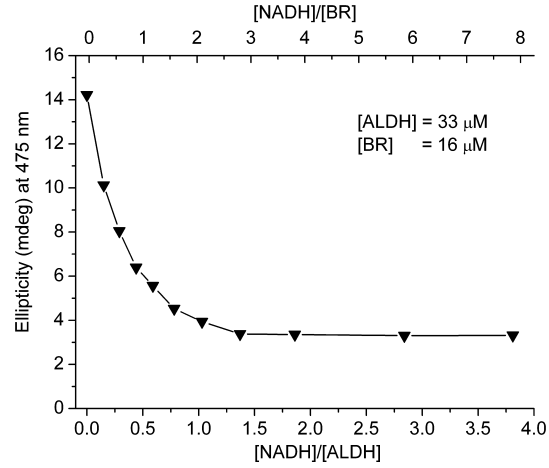

Figure 8. Effect of NADH on the positive ICD band of BR−ALDH complexes (Ringer buffer, $t = 25$ °C).

a distance of 20 Å below the molecular surface. The heme chromophore has a number of electronic transitions in the near-UV and VIS spectral regions, and because of the asymmetric protein environment these transitions are chirally perturbed so CTL exhibits a negative extrinsic CE ($\lambda_{max} = 394$ nm) associated with the Soret absorption band ($\lambda_{max} = 407$ nm).[31,32] This heme CD peak partially overlaps with the negative branch of the exciton couplet of BR bound to CTL, but it is well separated from the longer-wavelength positive CE (Figure 2). The profile of BR−CTL CD titration curves constructed from the negative and positive CD_{max} values of BR are very similar, suggesting that BR−heme binding interaction is less probable (data not shown). Besides the heme moiety, CTL also contains four coenzyme binding sites for NAD(P)H molecules at the surface of the enzyme.[33] The K_a values of human and bovine CTL for NADP were found to be $>10^8$ M^{-1}, and the enzyme binds NAD(H) with comparable affinity.[34] In most enzymes, NADP, NAD, and FAD usually adopt extended conformation, but in human and bovine liver CTL, NADPH is folded into a right-handed helix by rotation about its pyrophosphate linkage so that the adenine and nicotinamide rings are close but nearly at right angles to each other.[33,35] There is no direct interaction between the heme group and NADP; the closest approach between them is 13.7 Å. Free NADH molecules show a very weak intrinsic CD band >300 nm ($\Delta\varepsilon_{max}$ at 339 nm ≈ -0.3 M^{-1} cm^{-1}), which does not interfere with the CEs of BR. Upon addition of NADH to BR−CTL solution prepared at 0.3 molar ratio, magnitudes of both induced ellipticity bands decreased quickly to near-zero upon reaching equimolar [NADH]/[BR] ratio (Figure 7). In parallel, by the extinction of the ICD bands, the VIS absorption peak of BR displayed a large hypochromism indicating the aqueous aggregation of BR molecules displaced by NADH from the CTL binding site (at the end of the titration, $\varepsilon_{max} = 20\,000$ $M^{-1}cm^{-1}$ at 448.0 nm). Accordingly, the observed spectral changes are caused by a direct competitive interaction between NADH and BR molecules, and other possibilities such as the replacement of BR to another chirally nonspecific CTL binding site can be excluded. The proposed function of CTL-bound NADPH is that it prevents the inactivation of CTL,[33] so its replacement by BR may alter the enzyme activity.

Similarly to CTL, yeast ALDH is also composed of four identical subunits, each of which has one NADH-binding site and one firmly bound zinc atom, which is essential for catalysis.[36] At pH 7.5, the coenzymes bind with a moderate affinity ($K_a \approx 3 \times 10^4$ M^{-1}).[36] Distinctly from CTL, the ALDH-bound NADH molecules adopt extended conformation; that is, the adenine and nicotinamide rings are separated by at least 14 Å.[37] The addition of NADH to the 1:2 mixture of BR−ALDH solution abruptly decreased both the negative and the positive CE of BR, but above [NADH]/[ALDH] = 1 and [NADH]/[BR] = 2, no further intensity loss was observed (Figure 8). The starting ICD activity ([NADH] = 0) was reduced by 75%, and the spectroscopic profile of the residual CEs measured at the end of the titration were highly similar to that of the original bands (spectra not shown). The decrease in the ε_{max} value from 42 000 (446.0 nm) to 21 000 $M^{-1}cm^{-1}$ (442.2 nm) during the titration refers to the aqueous aggregation of BR molecules dissociated from the ALDH binding sites. These results indicate binding competition between NADH and BR for a common binding site on ALDH.

GLDH is ubiquitous in most organisms, having a pivotal role in the balance between nitrogen assimilation and amino acid catabolism. The homohexameric GLDH is allosterically regulated by a wide array of ligands such as GTP, NADH, and steroid hormones.[38,39] It is important to note that NAD(P)H binding induces significant conformational changes of GLDH, which are important in its complex allosteric regulation.[38−40] The CD spectrum of BR−GLDH solution displays the characteristic bisignate shape (Figure 4). Astonishingly, when aliquots of NADH stock solution were added to the sample, the CEs were gradually inverted (Figure 4). Magnitudes of the inverted CD bands were approximately three times the original values, and they were shifted to longer wavelengths by ~20 nm. These large CD changes were accompanied by only minor alterations in the absorption spectrum: λ_{max} of the VIS absorption peak showed a small, ~6 nm bathochromic shift, and the integrated areas under the curves at the beginning and at the end of the titration are nearly equal (Figure 4). The $P \rightarrow M$ helical inversion of the GLDH-bound BR upon addition of NADH is caused by a change in the stereochemistry of the pigment brought about by cobinding of the coenzyme to the protein. One possibility is that NADH displaces BR from its primary binding site to a secondary site at which the pigment binds with inverted *M*-helical conformation. However, this explanation is unlikely because the sign of the ICD bands showed no inversion when GLDH alone was titrated with BR from BR/GLDH molar ratios of 1:2 to 2:1 (data not shown). Therefore, a more obvious reason is that NADH binding causes chiral inversion of the bound BR by changing the internal topography of the BR binding site in such a way that the opposite, *M*-helicity conformer will

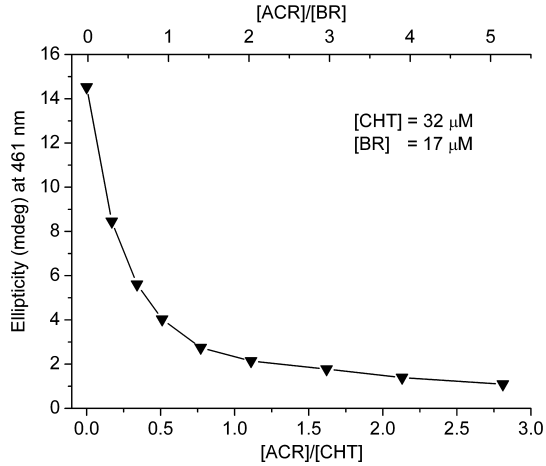

Figure 9. Effect of NADH on the negative ICD band of BR−CHT complexes (Ringer buffer, $t = 25$ °C). For clarity, absolute CD values were used.

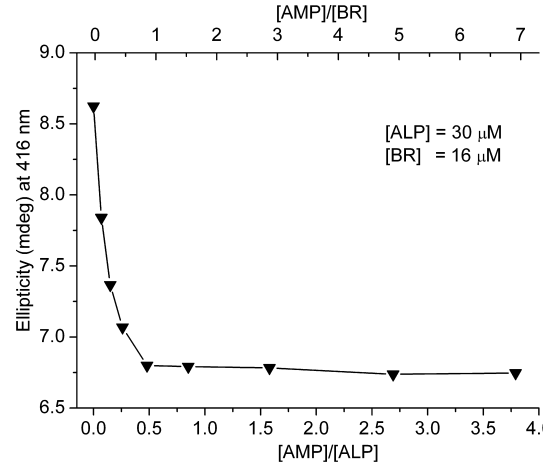

Figure 10. Effect of AMP on the negative ICD band of BR−ALP complexes (Ringer buffer, $t = 25$ °C). For clarity, absolute CD values were used.

preferentially be bound. The allosterically modified BR binding site exhibits greater conformational stereoselectivity than the original one, as reflected by the more intense exciton CEs measured in the presence of NADH (Figure 4).

It is well known that acridine dyes are competitive inhibitors of CHT because they bind to the substrate binding site (S1 pocket) of the enzyme in a one-to-one fashion.[41−43] Acridine (ACR) was selected to perform CD displacement measurements to investigate whether the S1 pocket of CHT is involved in the BR binding. Upon the addition of the dye into BR−CHT solution prepared at a 1:2 molar ratio, amplitudes of the induced CEs promptly decreased to near-zero in conjuction with the reduction of VIS ε_{max} value of BR by ~10 000 M^{-1} cm^{-1}, which refers to a direct ACR−BR binding competition in the S1 pocket (Figure 9). TRP and CHT have very similar tertiary structures, although they recognize different substrates.[44] Curiously, whereas CHT does bind BR (Figure 3), the BR−TRP mixture displayed no CD signals above 300 nm (data not shown). Intensity (ε_{max} ≈ 30 000 M^{-1} cm^{-1}), shape, and λ_{max} values (~443 nm) of the VIS absorption bands of BR measured with 35 μM TRP and in protein-free buffer solution were close to each other, indicating aqueous aggregation of the pigment molecules in the presence of TRP as well. Accordingly, these results rule out the possibility of accommodation of BR in a CD inactive binding site of TRP. The sharp contrast of the BR binding abilities of these closely related proteases may refer to subtle structural differences between the substrate binding pockets that can sensitively be detected by the presence or the total absence of induced exciton CD signals. BR used in 10 μM concentration has been reported to show 61% inhibition for the proteolytic activation of α-chymotrypsinogen A to chymotrypsin in a system containing 1 μg/mL (0.04 μM) TRP and 1 μg/mL chymotrypsinogen.[13] Because of the very high molar excess of BR, however, specificity of that inhibition is strongly questioned.

Among the three tissue-specific human ALPs, physiological role of the placental isozyme remains unclear. The dimeric placental ALP contains a peripheral site located 28 Å away from the catalytic pocket where 5′-AMP can bind.[45] The addition of AMP resulted in a prompt, small intensity reduction of both CEs of BR−ALP complexes together with the moderate decrease in the ε_{max} value (ε_{max} from ~48 000 at 457.2 nm to 38 000 M^{-1} cm^{-1} at 462.4 nm), which might be the consequence of the reduction of BR binding affinity of ALP by an allosteric mechanism (Figure 10). Because the placental, germ cell, and intestinal ALPs are 90−98% homologous,[45] it is proposed that all of these enzymes can also bind BR.

Conclusions

By using CD spectroscopy, which is a sensitive tool to detect induced chirality of small molecules bound to asymmetric hosts, this study demonstrated the binding of BR to various enzymes, BR inhibition of which has been previously reported. Because of its favorable optical and stereochemical properties, BR is a well-suited natural CD spectroscopic label for exploring its own protein binding. It has been shown that beyond the detection of noncovalent BR−enzyme complexes, the CD method can also be used to estimate the binding parameters and for monitoring BR−ligand−enzyme binding interactions. Results of CD competition experiments indicated the involvement of either the coenzyme (ALDH, CTL) or the catalytic pocket (CHT) in the accommodation of BR. For the case of GLDH and ALP, changes of the ICD bands of BR obtained upon the addition of NADH or AMP suggested the formation of ternary complexes and allosteric interaction between BR and NADH/AMP binding sites. Catalase is unique among the BR binding enzymes studied here because besides its prosthetic heme group, it can also bind the acyclic tetrapyrrole BR noncovalently in the NADH binding pocket. These results together with previous data on the inhibitory effect of BR on NAD(P)H-dependent enzymes[11,21,22] raise an interesting possibility: the regulatory role of BR on enzymatic functions, which is mediated by competitive or allosteric BR−coenzyme binding interactions. It seems that BR can adopt a conformation that is reminiscent to that of the bound coenzyme. Thus, it is feasible to speculate that metabolic enzymes having a NAD(P)H-binding fold are potential BR binding proteins.

Acknowledgment. This work was supported by the research grant of OTKA K69213. Technical assistance by undergraduate student Dávid Józsvai is appreciated.

References and Notes

(1) Vitek, L.; Ostrow, J. D. *Curr. Pharm. Des.* **2009**, *15*, 2869–2883.
(2) Lighnter, D. A.; Wijekoon, W. M.; Zhang, M. H. *J. Biol. Chem.* **1988**, *263*, 16669–16676.
(3) Person, R. V.; Peterson, B. R.; Lightner, D. A. *J. Am. Chem. Soc.* **1994**, *116*, 42–59.
(4) Blauer, G. *Isr. J. Chem.* **1983**, *23*, 201–209.

(5) Petersen, C. E.; Ha, C. E.; Harohalli, K.; Feix, J. B.; Bhagavan, N. V. *J. Biol. Chem.* **2000**, *275*, 20985–20995.
(6) Patra, S. K.; Pal, M. K. *Eur. J. Biochem.* **1997**, *246*, 658–664.
(7) Khan, M. M.; Muzammil, S.; Tayyab, S. *Biochimie* **2000**, *82*, 203–209.
(8) Pu, Y. M.; McDonagh, A. F.; Lightner, D. A. *J. Am. Chem. Soc.* **1993**, *115*, 377–380.
(9) Woolley, P. V., III; Hunter, M. J.; Arias, I. M. *Biochim. Biophys. Acta* **1976**, *446*, 115–123.
(10) Blauer, G. *Biochim. Biophys. Acta* **1986**, *884*, 602–604.
(11) Karp, W. B. *Pediatrics* **1979**, *64*, 361–368.
(12) Vaz, A. R.; Delgado-Esteban, M.; Brito, M. A.; Bolanos, J. P.; Brites, D.; Almeida, A. *J. Neurochem.* **2010**, *112*, 56–65.
(13) Qin, X. *Gut* **2007**, *56*, 1641–1642.
(14) McLoughlin, D. J.; Howell, M. L. *Biochim. Biophys. Acta* **1987**, *893*, 7–12.
(15) Simons, P. C.; Jagt, D. L. *J. Biol. Chem.* **1980**, *255*, 4740–4744.
(16) Ernster, L.; Zetterström, R. *Nature* **1956**, *178*, 1335–1337.
(17) Kamisaka, K.; Gatmaitan, Z.; Moore, C. L.; Arias, I. M. *Pediatr. Res.* **1975**, *9*, 903–905.
(18) Hansen, T. W.; Mathiesen, S. B.; Walaas, S. I. *Pediatr. Res.* **1996**, *39*, 1072–1077.
(19) Hansen, T. W. *Clin. Perinatol.* **2002**, *29*, 765–778.
(20) Rigato, I.; Ostrow, J. D.; Tiribelli, C. *Trends Mol. Med.* **2005**, *11*, 277–283.
(21) Flitman, R.; Worth, M. H., Jr. *J. Biol. Chem.* **1966**, *241*, 669–672.
(22) Yamaguchi, T. *J. Biochem.* **1970**, *68*, 441–447.
(23) Zsila, F.; Bikádi, Z.; Simonyi, M. *Biochem. Pharmacol.* **2003**, *65*, 447–456.
(24) Ostrow, J. D.; Mukerjee, P.; Tiribelli, C. *J. Lipid Res.* **1994**, *35*, 1715–1737.
(25) Blauer, G.; Harmatz, D.; Snir, J. *Biochim. Biophys. Acta* **1972**, *278*, 68–88.
(26) Tayyab, S.; Khan, N. J.; Khan, M. A.; Kumar, Y. *Int. J. Biol. Macromol.* **2003**, *31*, 187–193.
(27) Zsila, F.; Matsunaga, H.; Bikádi, Z.; Haginaka, J. *Biochim. Biophys. Acta* **2006**, *1760*, 1248–1273.
(28) Beuckmann, C. T.; Aoyagi, M.; Okazaki, I.; Hiroike, T.; Toh, H.; Hayaishi, O.; Urade, Y. *Biochemistry* **1999**, *38*, 8006–8013.
(29) Zsila, F. *FEBS Lett.* **2003**, *539*, 85–90.
(30) Boiadjiev, S. E.; Lightner, D. A. *Monatsh. Chem.* **2005**, *136*, 489–508.
(31) Blauer, G. *Struct. Bonding (Berlin, Ger.)* **1974**, *18*, 69–129.
(32) Kajiyoshi, M.; Anan, F. K. *J. Biochem.* **1977**, *81*, 1319–1325.
(33) Kirkman, H. N.; Gaetani, G. F. *Trends Biochem. Sci.* **2007**, *32*, 44–50.
(34) Kirkman, H. N.; Gaetani, G. F. *Proc. Natl. Acad. Sci. U.S.A.* **1984**, *81*, 4343–4347.
(35) Fita, I.; Rossmann, M. G. *Proc. Natl. Acad. Sci. U.S.A.* **1985**, *82*, 1604–1608.
(36) Trivic, S.; Leskovac, V. *J. Serb. Chem. Soc.* **2000**, *65*, 207–227.
(37) Ramaswamy, S.; Kratzer, D. A.; Hershey, A. D.; Rogers, P. H.; Arnone, A.; Eklund, H.; Plapp, B. V. *J. Mol. Biol.* **1994**, *235*, 777–779.
(38) Smith, T. J.; Stanley, C. A. *Trends Biochem. Sci.* **2008**, *33*, 557–564.
(39) Smith, T. J.; Peterson, P. E.; Schmidt, T.; Fang, J.; Stanley, C. A. *J. Mol. Biol.* **2001**, *307*, 707–720.
(40) Peterson, P. E.; Smith, T. J. *Structure* **1999**, *7*, 769–782.
(41) Marty, A.; Bourdeaux, M.; Dell' Amico, M.; Viallet, P. *Photochem. Photobiol.* **1984**, *40*, 175–183.
(42) Bernhard, S. A.; Lee, B. F.; Tashjian, Z. H. *J. Mol. Biol.* **1966**, *18*, 405–420.
(43) Wallace, R. A.; Kurtz, A. N.; Niemann, C. *Biochemistry* **1963**, *2*, 824–836.
(44) Tong, L.; Wengler, G.; Rossmann, M. G. *J. Mol. Biol.* **1993**, *230*, 228–247.
(45) Llinas, P.; Stura, E. A.; Menez, A.; Kiss, Z.; Stigbrand, T.; Millan, J. L.; Le Du, M. H. *J. Mol. Biol.* **2005**, *350*, 441–451.

BM1012103